Langmuir
Letter
pubs.acs.org/Langmuir


# Capillary Negative Pressure Measured by Nanochannel Collapse

Niels R. Tas,*[,†] Maryana Escalante,[†,§] Joost W. van Honschoten,[†] Henri V. Jansen,[†] and M. Elwenspoek[†,‡]

[†]*Transducers Science and Technology Group, MESA+ Institute for Nanotechnology and IMPACT Institute of Mechanics, Processes and Control, University of Twente, P.O. Box 217, 7500 AE Enschede, The Netherlands and* [‡]*FRIAS, University of Freiburg, Albertstrasse 19, D-79194 Freiburg, Germany.* [§]*Current affiliation: Biophysical Engineering Group, MESA+ Institue for Nanotechnology, University of Twente, P.O. Box 217, 7500 AE Enschede, The Netherlands*

*Received September 27, 2009. Revised Manuscript Received December 2, 2009*

A new method is presented to measure capillarity-induced negative pressure. Negative pressures of several bars have been measured for five different liquids (ethanol, acetone, cyclohexane, aniline, and water) over a range of surface tension. Capillary negative pressure was measured in 79 ± 3 nm silica nanochannels on the basis of the determination of the critical channel width for elastocapillary collapse of the flexible plate covering the channels. The results are consistent with the Young−Laplace equation.

## Introduction

Liquids can withstand considerable tension (negative pressure) because of the cohesive forces between the molecules. Reports by some of the greatest scientists of all time, namely, Huygens[1] and Newton,[2] about liquids under tension date back to the late 17th and early 18th centuries. The first notion that capillary action in narrow tubes can induce tension in a liquid was probably obtained by Kelvin when he derived what is now known as the Kelvin equation.[3] Experimental proof of the existence of capillary negative pressure was provided by Wiig and Juhola[4] through the measurement of a reduced density of water condensed in nanoporous activated charcoal, though quantitative interpretation was hampered by the unknown compressibility of water in the negative pressure regime as well as by a lack of exact knowledge of the pore diameter.

Despite its relevance in, for example, the understanding of the properties of water in unsaturated soil capillaries,[5] systematic experimental studies of capillary negative pressure are scarce. Measured pull-off forces in a surface forces apparatus and an atomic force microscope[6,7] confirm the extistence of large capillary negative pressures in nanometric gaps. However, the conversion from forces to pressures requires the application of the Kelvin equation and introduces inaccuracy. Elastocapillary deformation of silicon-based nanochannels was recently introduced and applied to measure capillary negative pressure in water.[8] Because bulk liquid can be easily introduced and observed, nanochannel-based methods do not rely on the condensation of the liquid and an estimation of the Kelvin radius to measure the negative Laplace pressure.

In this letter, we introduce a new method, based on elastocapillary collapse and the subsequent stiction of nanochannels to measure capillary negative pressure. The method is applied to five different liquids over a range of surface tension: ethanol, acetone, cyclohexane, aniline, and water. The existence of capillary negative pressure can be confirmed for all of these liquids and is consistent with the Young−Laplace equation.

Consider the capillary action in a thin rectangular capillary (height $h_0 \ll$ width $2w \ll$ length $L_0$), partially filled with liquid (Figure 1). Neglecting the meniscus curvature in the lateral plane, the pressure of the liquid phase $p_{liq}$ is given by $p_0 - 2\gamma \cos(\theta)/h$, where $h$ is the channel height near the meniscus, $\gamma$ the surface tension of the liquid, and $\theta$ is the contact angle of the liquid with respect to the channel walls. For water partially filling a hydrophilic channel, capillary negative pressure will occur when the channel height is below approximately 1 $\mu$m.

## Experimental Section

Measurements of capillary negative pressure were carried out in hydrophilic nanochannels (1 cm in length) with an initial height of $h_0 = 79 \pm 3$ nm and capped with an elastic membrane. The fabrication process has been presented in detail in ref 9. In summary, nanochannels were fabricated in arrays of different widths ranging from 2 to 10.5 $\mu$m in steps of 0.5 $\mu$m. The channel height was determined by the thickness of a silicon oxide spacer layer (grown by dry oxidation at 1100 °C) that was patterned by photolithography and 1% HF etching to define the nanochannels. Access holes connecting to the nanochannels through microchannels are included for the fluid supply. The channels were covered with an elastic membrane consisting of a silicon nitride−silicon oxide composite layer (Figure 2), which was transferred by fusion bonding a second wafer (carrying the membrane) to the first wafer (carrying the channel pattern). Before bonding, both wafers were cleaned, first in $HNO_3$ solution and then in $H_2O_2$/$H_2SO_4$ (1:3 at 130 °C, "piranha") to ensure a hydrophilic surface. ***Warning: Piranha and $HNO_3$ solutions should be handled with care.*** The wafer pair was annealed in a furnace ($N_2$) at 1100 °C for 2 h. Finally, the second support wafer was removed by reactive ion etching in $SF_6$ plasma at room temperature.

*Corresponding author. E-mail: n.r.tas@utwente.nl.

(1) Huygens, C. *Philos. Trans.* **1672**, *7*, 5027.
(2) Newton, I. *Optics*, 3rd ed.; London, 1721.
(3) Lord Kelvin, *Proc. R. Soc. Edinburgh* **1870**, *7*, 63.
(4) Wiig, E. O.; Juhola, A. J. *J. Am. Chem. Soc.* **1949**, *71*, 561.
(5) Mercury, L.; Tardy, Y. *C. R. Acad. Sci., Ser. IIa: Sci. Terre Planetes* **1997**, *325*, 947.
(6) Fisher, L. R.; Israelachvili, J. N. *Chem. Phys. Lett.* **1980**, *76*, 325.
(7) Yang, S. H.; Nosonovski, M.; Zhang, H.; Chung, K.-H. *Chem. Phys. Lett.* **2008**, *451*, 88.
(8) Tas, N. R.; Mela, P.; Kramer, T.; Berenschot, J. W.; van den Berg, A. *Nano Lett.* **2003**, *3*, 1537.
(9) van Honschoten, J. W.; Escalante, M.; Tas, N. R.; Jansen, H. V.; Elwenspoek, M. *J. Appl. Phys.* **2007**, *101*, 094310.

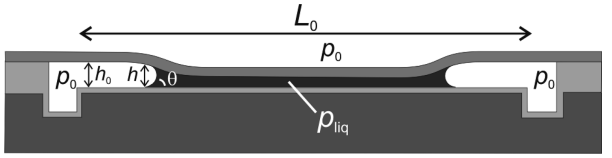


**Figure 1.** Schematic longitudinal section of a partially filled deformable nanochannel. The channel height near the meniscus is $h$.

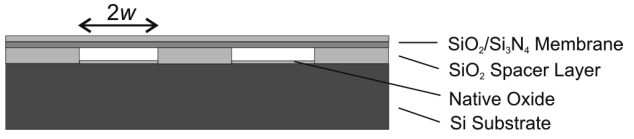


**Figure 2.** Schematic cross section of the nanochannel structure covered by a $SiO_2/Si_3N_4$ membrane.

Liquid was introduced into the chips by depositing droplets (5 $\mu$L) onto the access holes. Chips would then fill through capillary action, first through the microchannel and then through the nanochannels. Figure 3a shows a typical still image of the filling of the nanochannel array. Different liquids covering a rather wide range of surface tension were introduced in a total of 10 chips (2 chips for each liquid): water (Milli-Q, specific resistance 18 MΩ·cm), ethanol (Merck, VLSI Selectipur, 99.8%), acetone (VLSI Selectipur, 99.5%), cyclohexane (Merck, pro analysis, 99.5%), and aniline (Sigma-Aldrich, ACS reagent, 99%). Experiments were carried out at room temperature (20 ± 2 °C). Contact angles with respect to the channel walls for partially wetting liquids aniline and water were determined on reference wafers covered by native oxide and silicon nitride, respectively, which underwent the same cleaning procedure and heat treatment as the device wafers. Afterwards, filling chips were left to dry in the open air, which, depending on the vapor pressure of the liquid, would take several minutes up to several hours.

## Results and Analysis

In the filling and drying experiments, the liquid plugs were remarkably stable and cavitation was not observed. This can be explained by the fact that the critical radius for cavitation $R \approx -2\gamma/p$ [10] (with $p$ the negative pressure) for capillarity-induced negative pressure is larger than the characteristic dimensions of the capillary.[8]

In the wetted part of the partially filled channel, the plate deflects downward under the negative pressure load. Channels wider than a certain critical half width $w_c$ fully collapse (i.e., the cover plate touches the bottom of the channel). During filling, complete collapse occurs only across part of the filled length because there exists a pressure gradient from $p_0$ at the channel entrance down to the maximum negative pressure just behind the moving meniscus. For channel widths below $2w_c$, it was observed that with increasing channel width and thus decreasing plate stiffness the peculiar deformation of the meniscus shape related to the downward deflection of the plate[8] became increasingly prominent (Figure 3b). A detailed model explaining the observed shape and its relation to the capping deflection (for small deflections) is given by van Honschoten et al.[11]

To quantify the capillary negative pressure based on the full collapse of the capping plate, we focus the analysis on the drying process. This process is slow enough to be considered quasi-static, for which an energy-minimization procedure can be followed to predict the equilibrium states. During drying, liquid plugs are formed with a slowly receding meniscus at both ends. The full negative pressure as indicated by the Young−Laplace equation now acts across the whole wetted channel length. For channel widths smaller than $2w_c$, the capping plate recovers after the removal of the negative pressure load (after passage of the receding meniscus), and for channel widths larger than $2w_c$, removal of the pressure load in principle results in permanent adhesion of the plate to the bottom of the channel. In practice, because the critical width for collapse ($2w_c$) is close to the critical width for adhesion ($2w_a$), channels that fully collapsed did not always show adhesion across their entire length. Because partial adhesion is still indicative of collapse, we determined the critical width for collapse to be the average width of the last channel showing adhesion across part of its length and the first channel showing no adhesion at all. Adhesion could be easily detected by standard optical microscopy in bright-field mode (Figure 3c). After the determination of $w_c$ and the realization that at the critical width the center deflection is exactly equal to $h_0$, a mechanical analysis was carried out to determine the capillary negative pressure that induced the deflection.

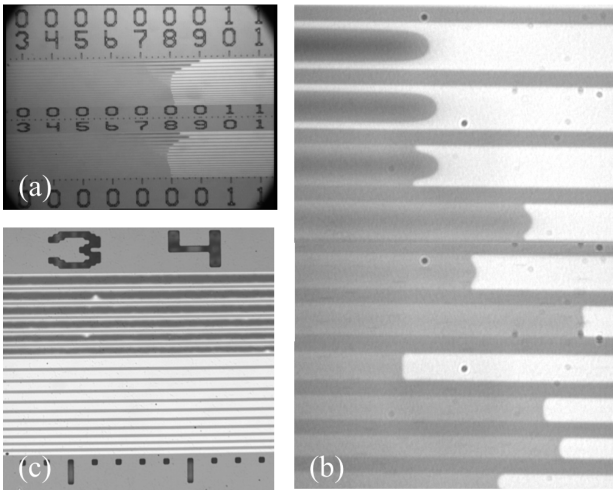


**Figure 3.** (a) Typical still image of the capillary filling of nanochannels (ethanol) of various widths varying from $2w$ = 2 to 10.5 $\mu$m (top view). The large ticks represent a distance of 100 $\mu$m. (b) Change in the shape of the meniscus with increasing channel width during filling (ethanol).[11] The channel width increases from 3 $\mu$m (bottom channel) to 7 $\mu$m (top channel). (c) Microscope image of a channel array after drying (water). Adhesion of the membrane to the channel bottom can clearly be distinguished by the dark color.

The analysis is complicated by the fact that for channel widths close to $2w_c$ the remaining liquid plugs detach from the side walls and only the central (and lowest) part of the channel is wetted; see Figure 4. Because the width $2b$ of the liquid plugs is unknown, we follow an energy-minimization procedure (for fixed liquid volume $V$) in which the center deflection $\delta$ of the capping and the plug width $2b$ are free variables. The total free energy of the system equals the sum of the mechanical deformation energy and the surface free energy of the partially wetted channel

$$F(\delta, b) = \frac{1}{2}k\delta^2 L(\delta, b) - 4bL(\delta, b)\gamma \cos(\theta) \qquad (1)$$

where $L(\delta, b)$ is the length of the liquid plug and $k$ is a constant that depends on the elastic properties and the shape function of the capping plate. To find $k$, we analyzed the cylindrical bending of the plate under a pressure load $p(x)$ taking into account residual stress. The deflection $v(x)$ is found by solving $D\partial_x{}^4 v - S\partial_x{}^2 v = p(x)$ with

(10) Fisher, J. C. *J. Appl. Phys.* **1948**, *19*, 1062.
(11) van Honschoten, J. W.; Escalante, M.; Tas, N. R.; Elwenspoek, M. *J. Colloid Interface Sci.* **2009**, *329*, 133. Figure 3b is reprinted with permission from Elsevier (copyright 2009) .

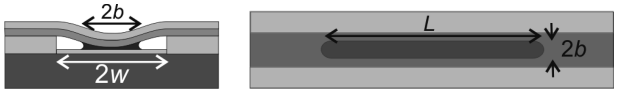


**Figure 4.** Channel cross section (left) and top view (right) defining the channel width $2w$, half the width of the liquid plug $b$, and the length of the liquid plug $L$.

the appropriate boundary conditions.[12] Here $D$ is the flexural rigidity of the composite membrane (per unit channel length) and $S = \Sigma\sigma_i t_i$ is the tensile force in the plate composed of layers having tensile stress $\sigma_i$ and thickness $t_i$.[13] For both a distributed load as well as for a point load, the solution can be written in the form of $v(x, u) = \delta(u)\Delta(x, u)$ where $\delta(u)$ is the center deflection ($x = 0$) and $\Delta(x, u)$ is a dimensionless shape function ($-w < x < w$).[14] The center deflection and shape function are both a function of the dimensionless parameter $u = w(S/D)^{1/2}$, which indicates whether the transverse stiffness is dominated by the bending stiffness or by the tensile stress in the plate.[14] For $u \approx 5$, which is the condition for the experiment, the shape function can be well approximated by $\Delta(x, u) = (1 - (x/w)^2)^2$, which is convenient for further calculations. We have followed an energy-minimization procedure based on eq 1 instead of solving the differential equation because the exact amplitude and distribution of the pressure load $p(x)$ are unknown. The plate stiffness $k$ can be found by calculating the strain energy for a given $\delta$ and the approximated shape function. Under the condition that $\partial_x v(x) \ll 1$, it follows that

$$\frac{1}{2}k(u)\delta^2 = \frac{1}{2}\delta^2\frac{25}{5}\frac{3}{f(u)D}{w^4} \tag{2}$$

where the plate stiffening $f(u)$ due to the net tensile stress in the plate is given by

$$f(u) = \left(1 + \frac{2}{21}u^2\right) \tag{3}$$

The average deflection in the wetted part of the channel is given by

$$\Gamma = \frac{\delta}{2b}\int_{-b}^{b}\Delta(u, x)\,\mathrm{d}x \tag{4}$$

For $\Delta(u, x) = (1 - (x/w)^2)^2$, we find $\Gamma(\delta, b) = \delta(1 - {}^2/_3(b^2/w^2) + {}^1/_5(b^4/w^4))$. The length of the liquid plug follows from

$$L(\delta, b) = \frac{V}{2b(h_0 - \Gamma(\delta, b))} \tag{5}$$

Equilibrium is analyzed by the minimization of $F(\delta, b)$ to $\delta$ and $b$ using eqs 2 and 5 for $k$ and $L$, respectively. This yields two equations $\partial F/\partial\delta = 0$ and $\partial F/\partial b = 0$ for three unknowns ($\delta$, $b$, and $w_c$). After taking $\delta = h_0$ for the center deflection at the critical channel width $w_c$, an equilibrium of $b = 0.61w$ is found and $\partial F/\partial\delta = 0$ (or $\partial F/\partial b = 0$) can be rewritten as

$$\frac{24h_0 f(u)D}{{w_c}^4} = \frac{2\gamma\cos(\theta)}{0.68h_0} \tag{6}$$

The left-hand side of the equation represents the mechanical pressure needed to induce a center deflection of $\delta = h_0$ (where the pressure would be acting across the complete width $2w$), and the right-hand side represents the capillary suction (pressure) that induces the bending. In the final state of drying $b = 0.61\ w$. Therefore, the actual Laplace pressure is larger by a factor of 1.11, as the meniscus height is 0.61 $h_0$ instead of 0.68 $h_0$.

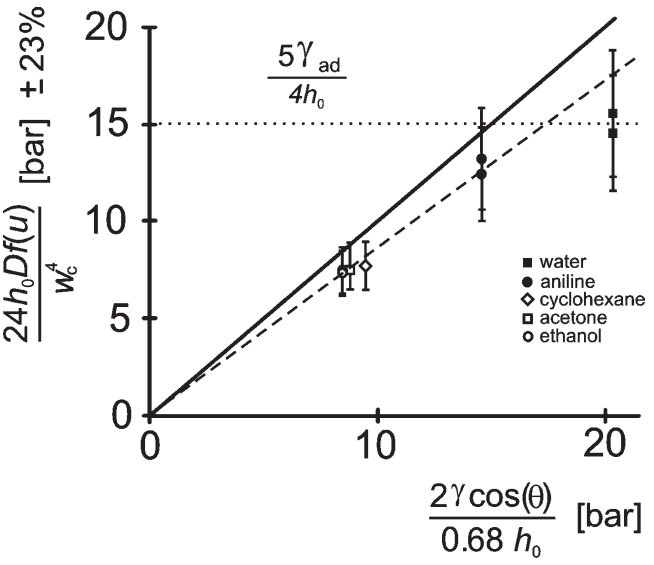


**Figure 5.** Measured and expected mechanical deformation pressure vs theoretical capillary suction. The expected relation is indicated by the solid line with a slope of 1, and the dashed line indicates the trend line in the experimental data.

Figure 5 shows the graphical representation of eq 6 based on the measured critical width for the different liquids with surface tension in the range of 20 to 73 mN m$^{-1}$. The expected relation between the mechanical deformation pressure and the capillary suction is indicated by the solid line with a slope of 1. The initial height $h_0 = 79 \pm 3$ nm is based on the thickness of the silicon oxide spacer layer. The flexural rigidity $D = (6.1 \pm 0.6) \times 10^{-11}$ N m is based on Young's modulus values of $70 \pm 10$ and $(2.6 \pm 0.1) \times 10^2$ GPa,[15] Poisson ratios of 0.17 and 0.27, and thicknesses of $79 \pm 3$ and $97 \pm 3$ nm for silicon oxide and silicon nitride layers in the plate, respectively. The plate stiffening $f(u)$ depends on the channel width and is estimated to range from $3.2 \pm 0.4$ for water up to $4.8 \pm 0.6$ for ethanol on the basis of a compressive stress of $0.30 \pm 0.05$ GPa for silicon oxide and a tensile stress of $1.2 \pm 0.1$ GPa for silicon nitride.[16] Because of the high tensile residual stress of the silicon nitride, the stiffening is independent of the plate deflection in the regime considered; therefore, the form ${}^1/_2k\delta^2$ for the deformation energy is adequate. For the surface tension of the liquids, we used tabulated values at 20 °C.[17] Static contact angle measurements on the reference wafers resulted in an effective $\cos(\theta) = 0.75 \pm 0.05$ for water and $\cos(\theta) = 0.91 \pm 0.04$ for aniline.[18] The other liquids (ethanol, cyclohexane, and acetone) are completely wetting. There is a possible systematic error of 23% in the mechanical pressure (12% in $f(u)D$ due to the residual stresses, 3% in $f(u)D$ due to the possible error in $D$, and 8% in ${w_c}^4$ due to the optical measurement of the channel width).

Figure 5 shows that for the lower and intermediate surface tension liquids the mechanical pressure is proportional to the surface tension. The slope of the trend line is 14% below the

(12) Timoshenko, S. P.; Woinowsky-Krieger, S. *Theory of Plates and Shells*; McGraw-Hill: New York, 1959; Chapter 1.
(13) The tensile stress in the silicon nitride is high; therefore, stiffening of the membrane due to deflection-induced stretching can be neglected.
(14) Tas, N.; Wissink, J. W.; Sander, L.; Lammerink, T.; Elwenspoek, M. *Sens. Actuators, A* **1998**, *70*, 171.
(15) Bouwstra, S. *Resonating Microbridge Mass Flow Sensor*. Ph.D. Thesis, University of Twente, **1990**; Chapter 3.
(16) Measured by the wafer curvature method after annealing.
(17) *CRC Handbook of Chemistry and Physics*, 67th ed.; Weast, R. C., Ed.; CRC Press: Boca Raton, FL, 1986; pp F32 − F33.
(18) Water: static contact angle of $\theta = 40 \pm 8°$ on silicon nitride and $\theta = 42 \pm 5°$ on silicon oxide. Aniline: static contact angle of $22 \pm 9°$ on silicon nitride and $28 \pm 5°$ on silicon oxide.

theoretical prediction, which in light of the possible systematic error is reasonable. For water, the highest surface tension liquid, the measured mechanical deformation pressure is somewhat below the trend line. This can be attributed to the fact that for water the critical width for collapse may be smaller than the critical width for adhesion, in which case the collapsed plate does not stay in contact with the channel bottom after complete evaporation of the liquid. An energy model for the adherence of the plate, expressing the balance between the adhesion energy and the mechanical deformation energy,[19,20] leads to the following equation for $w_a$:

$$\frac{24h_0 f(u)D}{{w_a}^4} = \frac{5\gamma_a}{4h_0} \quad (7)$$

In this representation, the limit of the presented measurement method can be indicated in Figure 5 by a horizontal line at a height of $^5/_4(\gamma_a/h_0)$. The dotted line indicates this limit based on the measured pressure of water. It corresponds to an adhesion energy of 0.10 J/m$^2$ for the adhesion of the plate, which is a reasonable value for the adhesion of the dehydroxylated silica surfaces.[19−21]

## Conclusions

We have presented a simple model based on energy minimization to describe the elastocapillary collapse of a nanochannel with flexible capping. By employing nanochannel collapse, we have measured capillary negative pressures for five different liquids in nanochannels of 79 nm height. The results are consistent with the presented model. The measured capillary negative pressures as expressed by $p_0 - 26.6h_0f(u)D/{w_c}^4$ amount to −7 bar for ethanol, −8 bar for cyclohexane and acetone, up to −13 bar for aniline, and −16 bar for water. The value for water is most likely a slight underestimate due to the limited adhesion strength. The consistency with the presented model is indicative for the validity of the Young−Laplace equation in the negative absolute pressure regime. The accuracy of the presented method can be improved by increasing the critical channel width through a thicker capping plate, which may also facilitate direct measurement of the capping stiffness.

It is anticipated that a better understanding of the phenomenon of capillary negative pressure can lead to new ways to avoid or reduce unwanted capillary collapse and subsequent adhesion (so-called stiction)[19,20] in microelectromechanical and nanoelectromechanical systems and to new insights in nanoscale contact mechanics.[22]

(19) Mastrangelo, C. H.; Hsu, C. H. *J. MEMS* **1993**, *2*, 33. Mastrangelo, C. H.; Hsu, C. H. *J. MEMS* **1993**, *2*, 44

(20) Tas, N.; Sonnenberg, T.; Jansen, H. V.; Legtenberg, R.; Elwenspoek, M. *J. Micromech. Microeng*. **1996**, *6*, 385.

(21) Legtenberg, R.; Tilmans, H. A. C.; Elders, J.; Elwenspoek, M. *Sens. Actuators, A* **1994**, *43*, 230.

(22) DelRio, F. W.; Dunn, M. L.; Phinney, L. M.; Bourdon, C. J.; de Boer, M. P. *Appl. Phys. Lett*. **2007**, *90*, 163104.